ELSEVIER

Journal of Power Sources 102 (2001) 118–123

JOURNAL OF POWER SOURCES

www.elsevier.com/locate/jpowsour

Pressure losses at dividing and combining junctions in a molten carbonate fuel cell stack

Haruhiko Hirata*, Takao Nakagaki, Michio Hori

Power and Industrial Systems Research and Development Center, Toshiba Corporation, 1, Toshiba-cho, Fuchu-shi, Tokyo 183-8511, Japan

Received 8 May 2000; received in revised form 17 January 2001; accepted 5 April 2001

Abstract

The pressure losses at manifold junctions in a molten carbonate fuel cell (MCFC) stack depend on the stacking positions of the cells and the flow rate in the manifold. These pressure losses affect the uniformity of gas flow rate in each stacked cell and consequently also affect the cell performance. In this study, the pressure losses at dividing and combining junctions in a plate heat-exchanger type MCFC stack were examined by numerical analysis. A stack consisting of 100 cells was assumed, and the junction pressure losses at various stacking positions of cells were calculated under various flow rate conditions ranging from the minimum possible flow rate (80% utilization of fuel gas) to the maximum possible flow rate (10% utilization of oxidant gas). The results were arranged according to the equations for loss coefficients, and were compared with the experimental results of previous studies.

Keywords: Molten carbonate fuel cell; Stack; Manifold; Numerical analysis; Pressure loss; Dividing junction; Combining junction

1. Introduction

In view of expectations regarding the high efficiency and low emission of nitrogen oxide etc. with direct conversion from chemical energy to electrical energy, the molten carbonate fuel cell (MCFC) is attracting attention as a power source for electric power, and development work aimed at realizing practical-use plant is progressing.

It is confirmed that the uniformity of gas distribution to each stacked cell has a big effect on the performance of the stack [1]. In the case of such a stack, when performing a calculation of gas distribution in each cell, the gas channels in the stack can be modeled as a multiple dividing and combining junction pipe arrangement consisting of the main-tubes modeling the supply and exhaust manifolds, and the branch tubes modeling the separator channels.

In such calculations, the dividing and combining pressure losses for the junctions of the supply and exhaust manifolds and separator channels are needed. Generally, the dividing and combining pressure losses for the junctions in the case that the main-tube Reynolds number is in the range of 10^4 to 10^5 have been widely investigated empirically for the pipe flow [2,3]. However, in the stack, the flow velocity in manifolds and separator channels and the flow-velocity ratio between manifolds and separator channels vary with the operation conditions and the stacking locations of cells, and in the cases of high-utilization fuel gas, Reynolds number in the manifolds can be less than 10^2. Therefore, in order to evaluate the flow rate distribution for the separator channel of each cell, it is necessary to grasp the detail of the dividing and combining pressure loss corresponding to the conditions of the flow velocity for the manifolds and separator channels and flow-velocity ratio between the manifolds and separator channels in the stack.

In this study, examination by numerical analysis was performed for the purpose of grasping the characteristic of the dividing and combining pressure loss in the junctions of manifolds and separator channels for the plate heat-exchanger type stack.

2. Stack configuration

The configuration of plate heat-exchanger type MCFC stack is shown in Fig. 1. Power generation is performed in the cells which consist of the electrolyte plate which contains molten carbonate as an electrolyte and the anode and cathode, and the fuel gas and oxidant gas are supplied to each cell by the separator channels. The fuel and oxidant gases are supplied to each separator channel via the supply manifold, and the gases are finally exhausted via the exhaust manifold.

* Corresponding author. Tel.: +81-42-333-2564; fax: +81-42-340-8060.
E-mail address: haruhiko.hirata@toshiba.co.jp (H. Hirata).

0378-7753/01/$ – see front matter
PII: S0378-7753(01)00790-X

Nomenclature

List of symbols

P	static pressure (Pa)
ΔP	pressure difference (Pa)
s	cross-sectional area for separator channel or branch tube (m^2)
S	cross-sectional area for manifold or main-tube (m^2)
u	mean flow velocity for separator channel or branch tube (m/s)
U	mean flow velocity for manifold or main-tube (m/s)

Greek letters

ρ	gas density (kg/m^3)
ζ	pressure loss coefficient

The manifolds which supply and exhaust gases in the cell stacking direction are arranged inside the separators as an internal manifold configuration, and this serves as the co-flow type stack in which the fuel and oxidant gases flow in the same direction to a cell in each separator channel. Therefore, the cross-section sizes of the manifolds are smaller than that of the external manifold configuration in which the manifolds are arranged outside the separators, and a prudent design is needed for uniform distribution of the fuel and oxidant gases to each cell in the stack.

3. Method of analysis

The finite volume method fluid analysis code PHOENICS and the body fitted coordinate (BFC) modeling method was used for the analysis. The analysis model is shown in Fig. 2.

The analysis model consists of the manifold and one of the separator channels which were stacked, and to evaluate dividing and combining pressure losses in the junctions of supply and exhaust manifold, the analysis in which the gas flow direction was changed as shown in the figure was performed.

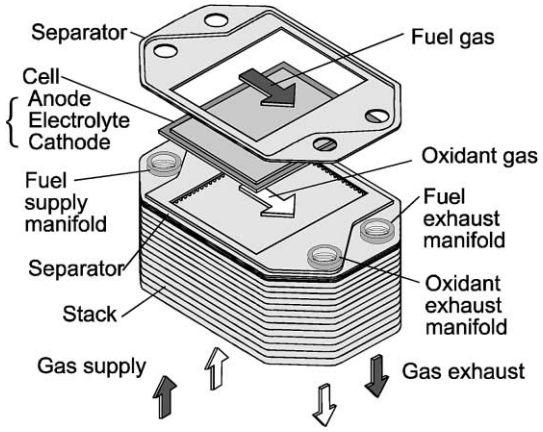

Fig. 1. Plate heat-exchanger type MCFC stack.

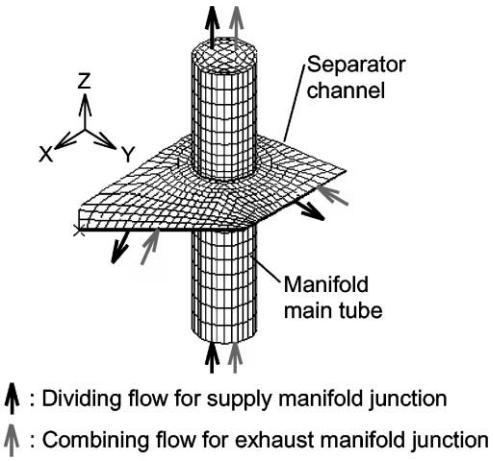

Fig. 2. Analysis model for manifold junctions.

The separator channel of the analysis model is a part of the separator channel of the stack, and the cut section was determined based on the uniform pressure section of flow analysis for the separator channels shown in Fig. 3a and b [4]. Here, Fig. 3a is for the 10% utilization oxidant flow, Fig. 3b is for the 80% utilization fuel flow, and the Reynolds number at the inlet portion are 1015 and 20, respectively. These pressure distributions were almost similar, although the difference of these Reynolds numbers are over 50 times. The other flow rate cases were ranging between these two cases, therefore the cut section of separator were applicable for the other analysis cases.

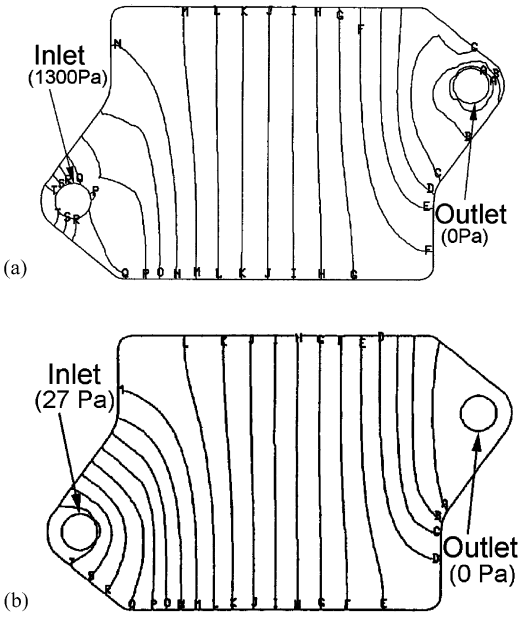

Fig. 3. (a) Pressure distribution in a separator channel (oxidant utilization = 10%); (b) pressure distribution in a separator channel (fuel utilization = 80%).

On the separator cut sections, free flow-out and flow-in conditions, which satisfy uniform pressure, were assumed for the dividing and combining junctions, respectively.

The manifold main-tubes whose lengths are three times and twice the diameter of the manifold were connected to the upstream and downstream of the separator channel, respectively. The manifold main-tube diameter and separator channel height were 0.12 and 3.5×10^{-3} m, respectively. The ratio of section areas S/s for the manifold main-tube cross-section area S and separator channel joint part cross-section area s was 8.57.

The analysis model has 19×22 BFC grids for the planar direction of the separator channel. For the height direction of the separator channel, it has 8 grids whose size varied in 1:2:3:4 between the nearest wall grid and the center grid for matching the parabolic flow-velocity distributions. For the cross-sectional direction of the manifold main-tube, it has 8×8 BFC grids whose size varied in 1:2:3:4 between the nearest wall grid and the center grid for matching the parabolic and 1/7th power low flow-velocity distributions. The manifold main-tubes on the upstream and downstream of the separator channel have 15 and 10 grids for the flow direction, respectively.

The parabolic and 1/7th power low flow-velocity distributions at the main-tube inlet port were adopted in the case that the main-tube Reynolds numbers was less than 2000 or over 2000. The k–ε turbulence model was adopted in the case that the main-tube Reynolds number was over 2000.

The principal flow analysis conditions are shown in Table 1.

Assuming a stack consists of 100 cells, the flow analysis was conducted for the flow rate conditions of 80, 20, and 10% utilizations for the fuel and 15 and 10% utilizations for the oxidant at the stacking positions for 1st, 10th, 30th, 60th, 80th, 90th, and 95th cells from the bottom.

Here, stacking positions correspond to the velocity ratios u/U of the separator channel junction mean flow-velocity u and manifold main-tube mean flow-velocity U, and u/U were 0.086, 0.094, 0.12, 0.21, 0.41, 0.78, and 1.4 for the stacking positions of 1st, 10th, 30th, 60th, 80th, 90th, and 95th, respectively.

The gas utilizations correspond to the separator channel junction mean flow-velocities u, and u were 0.64, 2.6, 5.2, 8.7, and 13 m/s for 80, 20, and 10% fuel utilizations, and 15 and 10% oxidant utilizations, respectively.

Where, Reynolds numbers of the manifold main-tube which uses the main-tube diameter and indraft average flow velocity U were from 4070 to 244 for $u = 0.64$ m/s, from 1600 to 976 for $u = 2.6$ m/s, from 3200 to 1950 for $u = 5.2$ m/s, from 13,500 to 8130 for $u = 8.7$ m/s, and from 203,000 to 12,200 for $u = 13$ m/s corresponding to the cases for u/U from 0.086 to 1.4, respectively.

Table 1
Principal flow analysis conditions

Inlet gas composition	
Fuel (H_2:CO_2:H_2O)	70:18:12
Oxidant (O_2:CO_2:N_2)	14:30:56
Current density (A/m^2)	1500
Active area (m^2)	0.9×0.9
Inlet gas temperature (K)	923
Pressure (MPa)	0.1
Gas density (kg/m^3)	
Fuel	0.150
Oxidant	0.436
Gas kinetic viscosity (m^2/s)	
Fuel	2.22×10^{-4}
Oxidant	8.99×10^{-5}

4. Results and discussions

The oxidant flow pressure-distributions of the dividing and combining flow for 10% utilization and $u/U = 0.086$ are shown in Fig. 4a and b, respectively.

The low-pressure domain before the junction and high-pressure domain after the junction were formed for the dividing flow, and the main-tube pressure after junction rises from the main-tube pressure before junction. The high-pressure domain before the junction and low-pressure domain after the junction were formed for the combining

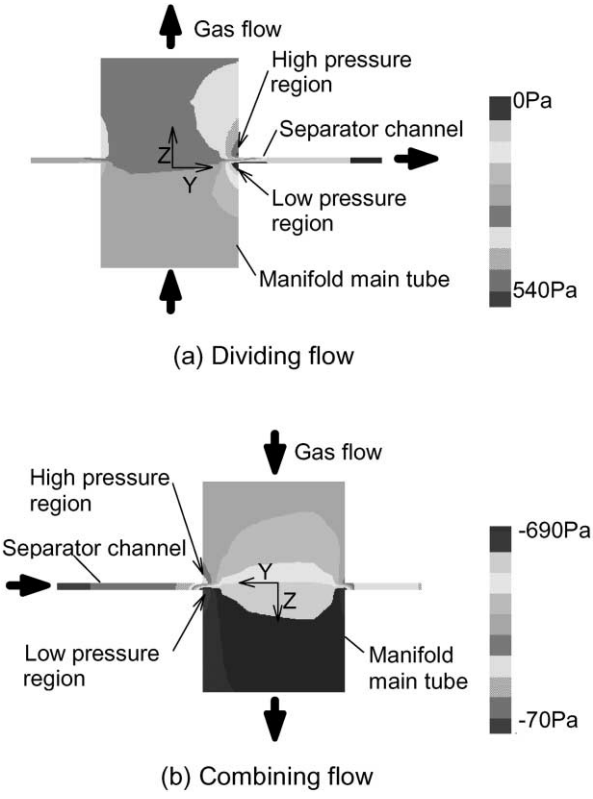

Fig. 4. Pressure distribution at the manifold junction (oxidant utilization = 10%, $u/U = 0.086$).

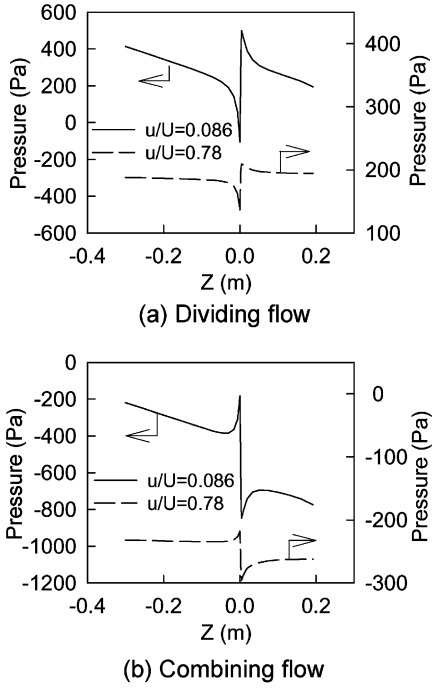

Fig. 5. Pressure distribution in the manifold main-tube (oxidant utilization = 10%).

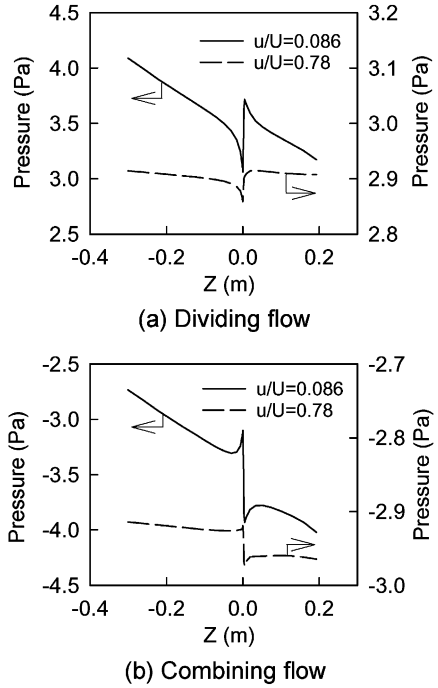

Fig. 6. Pressure distribution in the manifold main-tube (fuel utilization = 80%).

flow, and the main-tube pressure after junction declines from the main-tube pressure before junction. Generally, the rise of pressure in the main-tube flow for dividing junction passage and the fall of pressure in the main-tube flow for combining junction passage are well known [2], and the results of analysis were appropriate.

The pressure distributions on the main-tube wall for the dividing flow and the combining flow for the 10% utilization oxidant flow are shown in Fig. 5a and b, respectively. The pressure distributions on the main-tube wall for the dividing flow and the combining flow for the 80% utilization fuel flow are shown in Fig. 6a and b, respectively. Here, the axis of abscissa shows the main-tube stream orientation's distance which was measured from the separator channel undersurface.

The results for $u/U = 0.086$ corresponding to the 1st cell stacking position and $u/U = 0.78$ corresponding to the 90th cell stacking position are shown in each figure.

The main-tube pressure rise after the dividing junction and the main-tube pressure fall after the combining junction were larger in each case for $u/U = 0.086$ than that for $u/U = 0.78$. The pressure changes passing the junctions were larger for the combining flow than for the dividing flow in each case. Therefore, when these dividing and combining pressure losses are dominant for the pressure distribution formation of the manifold main-tubes of stack, it is anticipated that the variation of the main-tube pressure in the lower stacking part becomes larger than in the upper stacking part, and the pressure variation in the exhaust manifold becomes larger than in the supply manifold.

The main-tube pressures before and after junction, which are mentioned later, were determined by extrapolating based on the linear portions of pressure distributions on the manifold main-tube as a usual manner [2]. Therefore, effect of the local pressure rise and fall at the before and after junction, whose domain size became larger comparing the separator channel height, were eliminated on calculation of the pressure loss coefficients which are mentioned later.

The pressure loss coefficients which were obtained on the basis of the pressure distributions of the analysis results are shown in Fig. 7 for supply manifold junctions and in Fig. 8 for exhaust manifold junctions, as functions of u/U (i.e. the stacking position) and u (i.e. the utilization). The experiment results for the pipe channel flow for the ratios S/s of main-tube cross-sectional area S and branch-tube cross-sectional area s from 1.00 to 3.67 and the main-tube Reynolds numbers from 3×10^4 to 5×10^5 by Akiyama and Miura [3] are shown in each figure.

The definitions of pressure loss coefficients ζ_1 and ζ_2 for the supply manifold junctions and ζ_3 and ζ_4 for the exhaust manifold junctions are as follows:

$$\zeta_1 = \frac{\Delta P_1 - (\rho_1(u_1^2 - U_2^2))/2}{\rho_1 U_1^2/2} \tag{1}$$

$$\zeta_2 = \frac{\Delta P_2 - (\rho_1(U_2^2 - U_1^2))/2}{\rho_1 U_1^2/2} \tag{2}$$

$$\zeta_3 = \frac{\Delta P_3 - (\rho_2(U_4^2 - u_2^2))/2}{\rho_2 U_4^2/2} \tag{3}$$

$$\zeta_4 = \frac{\Delta P_4 - (\rho_2(U_4^2 - U_3^2))/2}{\rho_2 U_4^2/2} \tag{4}$$

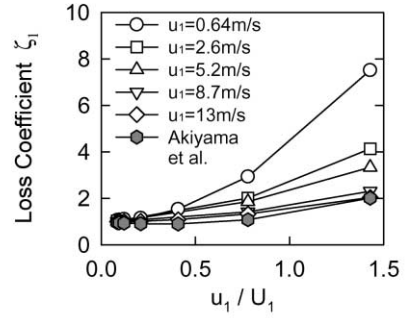

(a) Loss coefficient between the main tube before division and the separator channel

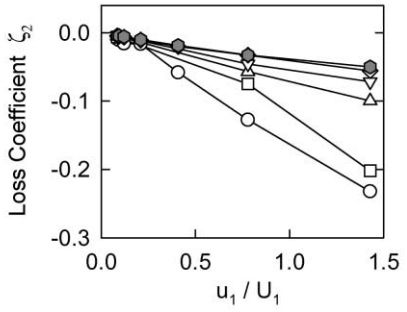

(b) Loss coefficient between the main tubes before and after division

Fig. 7. Loss coefficients for dividing junctions on supply manifold.

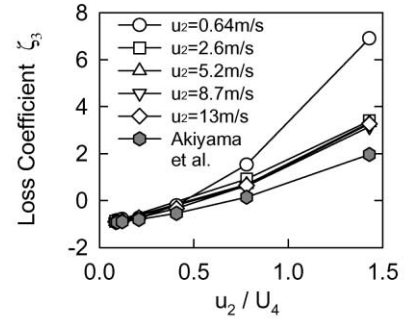

(a) Loss coefficient between the separator channel and the main tube after combination

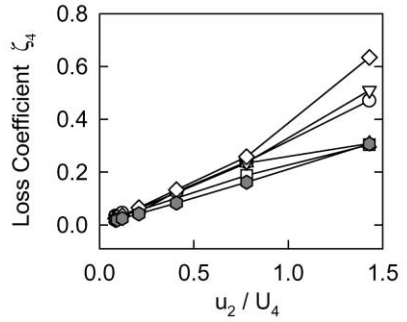

(b) Loss coefficient between the main tubes before and after combination

Fig. 8. Loss coefficients for combining junctions on exhaust manifold.

Here, ΔP_1 and ΔP_2 are the pressure differences for dividing junctions from upstream sides to downstream sides between the main-tubes before junction and separator channels, and between the main-tubes before junction and main-tubes after junction, respectively. The ρ_1 is gas density, and u_1, U_1, and U_4 are the mean flow velocity for the separator channel at the junction, and the manifold main-tube before the dividing, and after the dividing, respectively. The ΔP_3 and ΔP_4 are the pressure differences for combining junctions from upstream side to downstream side between the manifold main-tubes before junctions and separator channels, and between the manifold main-tubes before junctions and after junctions, respectively. The ρ_2 is gas density, and u_2, U_3, and U_4 are the mean flow velocity for the separator channel at the junction, and the manifold main-tube before the combining, and after the combining, respectively.

The pressure loss coefficients become negative value due to the pressure rise according to flow-velocity reduction passing the junction for ζ_2 and the dynamic-pressure change passing the junction for ζ_3.

Generally, the effect of the main-tube Reynolds number on the junction pressure loss is slight when the flow in the main-tube is in turbulence condition, and the effect of the cross-sectional area ratio on the dividing flow pressure loss is also slight [2].

In these analysis results, the loss coefficients ζ_1 and ζ_2 coincide with the experiment results of Akiyama and Miura [3] in each u_1/U_1, when $u_1 = 8.7$ m/s and 13 m/s, i.e. main-tube Reynolds numbers are over 8000 in the turbulence condition. However, the difference between analysis results and experiment results becomes larger as main-tube Reynolds numbers become smaller, and ζ_1 and ζ_2 become 3.7 times and 4.6 times larger values than the experimental results, respectively, when $u_1 = 0.64$ m/s and $u_1/U_1 = 1.4$.

Thus, when the main-tube Reynolds number is low, the junction pressure losses in the fuel cell stack cannot be estimated by using general empirical formulas with sufficient accuracy, and original estimation formulas are needed.

Since the conditions when the main-tube Reynolds number and u become small are equivalent to the conditions for the high-utilization fuel gas flow, it is important to know the junction pressure loss coefficients because of the large effect on the cell performance by the gas flow distribution for each cell in the stack.

With regard to combining junction pressure loss, it is known that the effect of the main-tube and a branch-tube cross-sectional area ratio on the loss coefficients becomes large, with the result that the pressure loss coefficients become larger as the cross-sectional area ratio becomes larger [2].

In these analysis results whose cross-sectional area ratio of 8.57 is larger than the 3.67 of the experiment of Akiyama and Miura [3], the loss coefficients ζ_3 become 3.5 times larger than those of the experimental results for $u_2 = 0.64$ m/s and $u_2/U_4 = 1.4$. The effects of Reynolds number on the loss coefficients are slight when u_2 are over

2.6 m/s, i.e. main-tube Reynolds number is more than 1000, and the loss coefficients are mutually in agreement in each u_2. The loss coefficients are larger than the former results, when a main-tube Reynolds number is $u_2 = 0.64$ m/s, i.e. main-tube Reynolds number is less than 800. The loss coefficients ζ_4 also become larger than the experimental results in accordance with the increase of u_2/U_4.

From the results shown in Fig. 7, the pressure loss coefficients ζ_1 and ζ_2 for the supply manifold junctions are arranged as follows in relation with u_1/U_1 and u_1, respectively.

$$\zeta_1 = 2.56\left(\frac{u_1}{U_1}\right)^{1.95} u_1^{-0.548} + 1.0 \quad (5)$$

$$\zeta_2 = -0.131\left(\frac{u_1}{U_1}\right)^{1.10} u_1^{-0.448} \quad (6)$$

From the results shown in Fig. 8, the pressure loss coefficients ζ_3 and ζ_4 for the exhaust manifold junctions are arranged as follows in relation with u_2/U_4 and u_2, respectively.

$$\zeta_3 = 3.72\left(\frac{u_2}{U_4}\right)^{1.68} u_2^{-0.152} - 1.0 \quad (7)$$

$$\zeta_4 = 0.411\left(\frac{u_2}{U_4}\right)^{1.12} u_2^{0.0628} \quad (8)$$

The normalized standard errors in parameter presumption of these formulas are 4.5, 7.5, 19, and 23% for the formula (5), (6), (7), and (8), respectively.

5. Conclusions

Regarding the gas flow in plate heat-exchanger type MCFC stack, the combining and dividing pressure losses in the junctions of manifold main-tube and separator channel were examined by numerical analysis, and the following results were obtained.

1. In the presumption of junction pressure loss coefficients for the gas flow in a MCFC stack, using the prior empirical formula causes considerable error because of the difference of Reynolds number for the dividing pressure losses and the difference of cross-sectional area ratio of a main-tube and a branch tube. Therefore, for the detailed gas flow distribution calculation, the original junction pressure loss presumption formulas are required.
2. On the basis of the analysis results, the pressure loss presumption formulas which match the gas flow conditions in a MCFC stack are obtained as functions of the branch-tube flow velocity and the flow-velocity ratio of branch tube and main-tube.

Acknowledgements

This work was conducted by the MCFC Research Association. The MCFC Research Association was commissioned to do the work by the New Energy and Industrial Technology Development Organization (NEDO) as a part of the New Sunshine Program of the Ministry of International Trade and Industry (MITI). We appreciate the advice and support of the MCFC Research Association, NEDO and MITI.

References

[1] H. Hirata, M. Hori, J. Power Sources 63 (1996) 115–120.
[2] The Japan Society of Mechanical Engineers, Data Book of Hydraulic Losses in Pipes and Ducts, JSME, Tokyo, 1989.
[3] I. Akiyama, K. Miura, Proc. JSME Annual Meeting 179 (1967) 65–68.
[4] H. Hirata, T. Nakagaki, M. Hori, J. Power Sources 83 (1999) 41–49.